Molecular Pharmacology Fast Forward. Published on September 10, 2004 as doi:10.1124/mol.104.002618
This article has not been copyedited and formatted. The final version may differ from this version.

UPREGULATION OF CYCLOOXYGENASE-2 EXPRESSION IS INVOLVED IN R(+)-METHANANDAMIDE-INDUCED APOPTOTIC DEATH OF HUMAN NEUROGLIOMA CELLS

Burkhard Hinz, Robert Ramer, Karin Eichele, Ulrike Weinzierl, Kay Brune

Department of Experimental and Clinical Pharmacology and Toxicology,

Friedrich Alexander University Erlangen-Nürnberg, Fahrstrasse 17, D-91054 Erlangen,

Germany

Running title: Role of COX-2 in neuroglioma cell death by R(+)-methanandamide

Corresponding author: Dr. Burkhard Hinz, Department of Experimental and Clinical Pharmacology and Toxicology, Friedrich Alexander University Erlangen-Nürnberg, Fahrstrasse 17, D-91054 Erlangen, Germany. Phone: +49-9131-8522754; Fax: +49-9131-8522774; E-mail: hinz@pharmakologie.uni-erlangen.de

Text pages (including Tables and Figure legends): 36

Figures: 8

Tables: 2

References: 40

Abstract word count: 247

Introduction word count: 654

Discussion word count: 1478

Abbreviations: AM-251, [N-(Piperidin-1-yl)-5-(4-iodophenyl)-1-(2,4-dichlorophenyl)-4-methyl-1H-pyrazole-3-carboxamide]; AM-630, [(6-Iodo-2-methyl-1-[2-(4-morpholinyl)ethyl]-1H-indol-3-yl) (4-methoxyphenyl)methanone]; CB_1, cannabinoid receptor 1; CB_2, cannabinoid receptor 2; COX, cyclooxygenase; C_2-ceramide, D-erythro-sphingosine; dihydro-C_2-ceramide, dihydro-N-acetyl-sphingosine; NSAID, non-steroidal anti-inflammatory drug; NS-398, [N-[2-(Cyclohexyloxy)-4-nitrophenyl]-methanesulfonamide]; PG, prostaglandin; PGE_2, prostaglandin E_2; R(+)-MA, R(+)-methanandamide (R-(+)-arachidonyl-1'-hydroxy-2'-propylamide); RT-PCR, reverse transcriptase-polymerase chain reaction; Δ^9-THC, Δ^9-tetrahydrocannabinol; siRNA, small-interfering RNA; VR_1, vanilloid

receptor 1; WST-1, (4-[3-(4-Iodophenyl)-2-(4-nitrophenyl)-2H-5-tetrazolio]-1.6-benzene disulfonate).

Abstract. Cannabinoids have been implicated in the reduction of glioma growth. The present study investigated a possible relationship between the recently shown induction of COX-2 expression by the endocannabinoid analogue, R(+)-methanandamide (R(+)-MA), and its effect on the viability of H4 human neuroglioma cells. Incubation with R(+)-MA for up to 72 h decreased the cellular viability and enhanced accumulation of cytoplasmic DNA fragments in a time-dependent manner. Suppression of R(+)-MA-induced prostaglandin (PG) E_2 synthesis with the selective COX-2 inhibitor celecoxib (0.01-1 μM) or inhibition of COX-2 expression by COX-2-silencing small-interfering RNA (siRNA) was accompanied by inhibition of R(+)-MA-mediated DNA fragmentation and cell death. In contrast, the selective COX-1 inhibitor SC-560 was inactive in this respect. Cells were also protected from apoptotic cell death by other COX-2 inhibitors (NS-398, diclofenac) and by the ceramide synthase inhibitor fumonisin B_1 which interferes with COX-2 expression by R(+)-MA. Moreover, the proapoptotic action of R(+)-MA was mimicked by the major COX-2 product PGE_2. Apoptosis and cell death by R(+)-MA were not affected by antagonists of CB_1-, CB_2- and VR_1 receptors. In further experiments, celecoxib was demonstrated to suppress apoptotic cell death elicited by anandamide which is structurally similar to R(+)-MA. Collectively, this study defines COX-2 as a hitherto unknown target by which a cannabinoid induces apoptotic death of glioma cells. Furthermore, our data show that pharmacological concentrations of celecoxib may interfere with the proapoptotic action of R(+)-MA and anandamide suggesting that co-treatment with COX-2 inhibitors could diminish glioma regression induced by these compounds.

Molecular Pharmacology Fast Forward. Published on September 10, 2004 as DOI: 10.1124/mol.104.002618
This article has not been copyedited and formatted. The final version may differ from this version.

INTRODUCTION

There is presently a renaissance in studying potential therapeutical effects of cannabinoids that exert a broad array of actions within the central nervous system as well as on immune, cardiovascular, respiratory, digestive, reproductive, and ocular functions. Although the antineoplastic activity of Δ^9-tetrahydrocannabinol (Δ^9-THC), the principal psychoactive component of marijuana, has been known since the 1970s (Munson et al., 1975), cannabinoids have been no more than some years ago associated with the management of malignant brain tumours. In this context cannabinoids have been shown to induce regression of malignant gliomas in rodents (Galve-Roperh et al., 2000). Different mechanisms have been proposed to account for the proapoptotic and antiproliferative effects of different cannabinoids on glioma cells (for review see Guzman et al., 2001). In rat C6 glioma cells, Δ^9-THC has been demonstrated to reduce cellular viability by a mechanism involving activation of cannabinoid receptors and sustained generation of ceramide (Galve-Roperh et al., 2000). On the other hand, a recent study suggests that the antiproliferative effects of the endocannabinoids anandamide and 2-arachidonoylglycerol in these cells are mediated by a mechanism involving combined activation of cannabinoid and vanilloid receptors (Jacobsson et al., 2001). Collectively, the results of these and other studies suggest that there is no universal mechanisms by which plant-derived, synthetic and endogenous cannabinoids affect cell viability and proliferation of glioma cells.

A relationship between cannabinoids and prostaglandins (PGs) has been established by several lines of evidence. Accordingly, various actions of cannabinoids within the central nervous system, including hippocampal neuronal death (Chan et al., 1998), dilation of cerebral arterioles (Ellis et al., 1995), psychoactive and behavioural effects (Burstein et al., 1989; Perez-Reyes et al., 1991; Yamaguchi et al., 2001) or reduction of intraocular pressure

Molecular Pharmacology Fast Forward. Published on September 10, 2004 as DOI: 10.1124/mol.104.002618
This article has not been copyedited and formatted. The final version may differ from this version.

(Green et al., 2001) have been associated with an increased production of PGs. Recent studies from our laboratory have shown that cannabinoids induce the expression of the cyclooxygenase-2 (COX-2) enzyme in human neuroglioma cells via a cannabinoid- and vanilloid receptor-independent pathway involving increased synthesis of ceramide (Ramer et al., 2001; Ramer et al., 2003). However, the functional consequence of COX-2 induction by cannabinoids in these cells has not been established so far.

COX-2, which is encoded by an immediate-early gene, catalyzes the first step of the synthesis of prostanoids (for review see Hinz and Brune, 2002). In recent years, COX-2 has been associated with cellular growth, survival and differentiation (for review see Gupta and DuBois, 2001; Chan et al., 2002; Subbaramaiah and Dannenberg, 2003). Thus, the induction of COX-2 expression by cannabinoids raises several questions referring to the viability of neuroglioma cells. As COX-2-derived PGs have been implicated to result in resistance of cancer epithelial cells to apoptosis (Tsujii and DuBois, 1995), it could be expected that cannabinoids diminish their antimitotic and proapoptotic action by virtue of their capacity to induce COX-2 expression. On the other hand, studies performed on neocortical (Bagetta et al., 1998) and amnion-derived cells (Moore et al., 1999) suggest that induction of the COX-2 signaling cascade may sensitize these cells to apoptotic death. Moreover and in line with a possible proapoptotic function of COX-2, inhibitors of this enzyme have recently been shown to attenuate the growth-inhibitory and proapoptotic effects of different chemotherapeutic agents on ovarian epithelial cancer (Munkarah et al., 2003) and mammary epithelial cancer cells (Na and Surh, 2002).

In the present study we therefore examined a possible relationship between the induction of the COX-2 pathway by the endocannabinoid analogue, R(+)-methanandamide (R(+)-MA), and its concomitant effect on the viability of H4 human neuroglioma cells. H4 cells represent an established epithelial-like neuroglioma cell line derived from a human brain tumor (Kim et

al., 2000; Krex et al., 2001; Jayanthi et al., 2001). Our results demonstrate a substantial induction of apoptosis and cell death by R(+)-MA that is mediated, at least in part, by COX-2-dependent PGs synthesized upon treatment of cells with R(+)-MA. Moreover, our data imply that co-treatment with selective COX-2 inhibitors could diminish glioma regression induced by cannabinoids.

Molecular Pharmacology Fast Forward. Published on September 10, 2004 as DOI: 10.1124/mol.104.002618
This article has not been copyedited and formatted. The final version may differ from this version.

MATERIALS AND METHODS

Materials.

AM-251, AM-630, anandamide, capsazepine, NS-398 and PGE_2 were purchased from Alexis Deutschland GmbH (Grünberg, Germany). C_2-ceramide, dihydro-C_2-ceramide, fumonisin B_1 and R(+)-MA were purchased from Calbiochem (Bad Soden, Germany). Bisbenzimide, diclofenac sodium and Δ^9-THC were obtained from Sigma (Deisenhofen, Germany). Dulbecco´s modified essential medium (DMEM) with 4 mM L-glutamine and 4.5 g/l glucose was from Cambrex Bio Science Verviers S.p.r.l. (Verviers, Belgium). Fetal calf serum and penicillin-streptomycin were obtained from PAN Biotech (Aidenbach, Germany) and Invitrogen (Karlsruhe, Germany), respectively.

Cell culture.

H4 human neuroglioma cells were maintained in DMEM supplemented with 10% heat-inactivated fetal calf serum, 100 U/ml penicillin and 100 µg/ml streptomycin. The cells were grown in a humidified incubator at 37°C and 5% CO_2. All incubations were performed in serum-free medium.

Quantitative RT-PCR analysis.

H4 neuroglioma cells were grown to confluence in 24-well plates. After incubation of cells with the respective test compounds or vehicle for the indicated times, supernatants were removed and cells were lysed for subsequent RNA isolation. Total RNA was isolated using the RNeasy total RNA Kit (Qiagen, Hilden, Germany). ß-Actin- (internal standard) and COX-2 mRNA levels were determined by quantitative real-time RT-PCR. Briefly, this method uses the 5´→3´exonuclease activity of the Taq polymerase to cleave a probe during PCR. A probe

consists of an oligonucleotide coupled with a reporter dye (6-carboxyfluorescein; 6FAM) at the 5´end of the probe and a quencher dye (6-carboxy-tetramethylrhodamine; TAMRA) at an internal thymidin. After cleavage of the probe, reporter and quencher dye become separated, resulting in an increased fluorescence of the reporter. Accumulation of PCR products was detected directly by monitoring the increase in fluorescence of the reporter dye using the integrated thermocycler and fluorescence detector ABI PRISM^{TM} 7700 Sequence Detector (Applied Biosystems, Darmstadt, Germany). Quantification of mRNA was performed by determining the threshold cycle (C_T), which is defined as the cycle at which the 6FAM fluorescence exceeds 10 times the standard deviation of the mean baseline emission for cycles 3 to 10. COX-2 mRNA levels were normalized to ß-actin according to the following formula: C_T (COX-2) – C_T (ß-actin) = ΔC_T. Subsequently, COX-2 mRNA levels were calculated using the $\Delta\Delta C_T$ method: ΔC_T (test compound) - ΔC_T (vehicle) = $\Delta\Delta C_T$ (test compound). The relative mRNA level for the respective test compound was calculated as $2^{-\Delta\Delta C_T}$ x 100%. RT-PCR reaction was performed using the One Step RT-PCR kit (Qiagen, Hilden, Germany). RNA samples were amplified using specific primers for human ß-actin and COX-2 (TIB MOLBIOL, Berlin, Germany) as described previously (Ramer et al., 2001).

Western blot analysis.

Cells grown to confluence in 10-cm dishes were incubated with test substance or vehicle for the indicated times. Afterwards, H4 neuroglioma cells were washed, harvested, and pelleted by centrifugation. Cells were than lysed in solubilization buffer (50 mM HEPES pH 7.4, 150 mM NaCl, 1 mM EDTA, 1% (v/v) Triton® X-100, 10% (v/v) glycerol, 1 mM phenylmethylsulfonyl fluoride, 1 µg/ml leupeptin and 10 µg/ml aprotinin), homogenized by sonication, and centrifuged at 10,000 x g for 5 min. Supernatants were used for Western blot analysis. Proteins were separated on a 10% sodium dodecyl sulfate-polyacrylamide gel.

Following transfer to nitrocellulose and blocking of the membranes with 5% milk powder, blots were probed with specific antibodies raised to COX-2 (BD Biosciences, Heidelberg, Germany) and COX-1 (Santa Cruz Biotechnologies, Inc., Heidelberg, Germany), respectively. Subsequently, membranes were probed with horseradish peroxidase (HRP)-conjugated Fab-specific anti-mouse IgG (Sigma, Deisenhofen, Germany). Antibody binding was visualized by enhanced chemiluminescence (ECL) Western blotting detection reagents (Amersham Pharmacia Biotech, Freiburg, Germany).

Determination of PGE_2.

H4 cells were seeded in 96-well flat bottom microplates at a densitiy of 5 x 10,000 cells/well and were grown to confluence. Thereafter, cells were incubated with the respective test compounds or its vehicles for the indicated times in 100 µl medium without serum. PGE_2 concentrations in cell culture supernatants were determined using a commercially available enzyme immunoassay kit (Cayman, Ann Arbor, MI, USA).

Cell viability analysis.

H4 cells were seeded in 96-well flat bottom microplates at a densitiy of 5 x 10,000 cells/well and were grown to confluence. Thereafter, cells were incubated with the respective test compounds for the indicated times in 100 µl medium without serum. In experiments exceeding a 24-h incubation period, new medium and test substance were added daily. Following the desired incubation time, cell viability was measured by the colorimetric WST-1 test (Roche Diagnostics, Mannheim, Germany). This cell viability test is based on the cleavage of the tetrazolium salt WST-1 (4-[3-(4-Iodophenyl)-2-(4-nitrophenyl)-2H-5-tetrazolio]-1.6-benzene disulfonate) by mitochondrial dehydrogenases in metabolically active cells.

Molecular Pharmacology Fast Forward. Published on September 10, 2004 as DOI: 10.1124/mol.104.002618
This article has not been copyedited and formatted. The final version may differ from this version.

Detection of DNA fragmentation.

H4 cells were seeded in 24-well plates at a densitiy of 1.5 x 100,000 cells/well and were grown to confluence. Thereafter, cells were incubated with the respective test compounds or its vehicles for the indicated times. Adherent cells were harvested by trypsinization and combined with the detached cells. Induction of apoptosis was assessed using the cell death detection ELISA^{PLUS} kit (Roche Diagnostics, Mannheim, Germany). This test is based on the detection of cytoplasmic histone-associated DNA fragments (mono- and oligonucleosomes), which are generated during apoptosis. ELISA was performed using 20,000 cells according to the manufacturer´s instructions. For detection of necrosis, histone-complexed DNA fragments were detected directly in the cell culture supernatant.

Detection of apoptotic nuclear morphology using bisbenzimide.

For detection of apoptotic nuclear morphology, cells grown to confluence in 35-mm dishes were incubated with test substance or vehicle for the indicated times. Afterwards, supernatants were removed and cells were washed and fixed in Carnoy's fluid for 30 min and stained with 100 ng/ml of bisbenzimide at room temperature for 10 min. After washing, cells were embedded under coverslips using glycerol (10%, Vol/Vol) and examined under a microscope equipped for epifluorescence illumination.

Construction of siRNA.

Small-interfering RNA (siRNA) against COX-2 was constructed as described by Elbashir et al. (2002) and synthesized by Qiagen (Qiagen GmbH, Hilden, Germany). The target sequence was 5´aactgctcaacaccggaattttt3´ (bases 291-313 of NM000963.1) The siRNA sequence was controlled via BLAST search and did not show any homology to other known human genes.

A negative (non-silencing) control siRNA against the target sequence 5´aattctccgaacgtgtcacgt3´ was purchased from Qiagen (cat. No. 1022076).

Transfections.

For DNA fragmentation assays or determination of COX-2 mRNA, cells were plated in 24-well plates and grown to 50-80% confluence. Thereafter, cells were transfected with COX-2-specific silencing siRNA or non-silencing siRNA using RNAiFect® (Qiagen GmbH, Hilden, Germany) as transfection reagent, following the manufacturer`s instructions. Briefly, for each well 1 µg COX-2 siRNA or non-silencing siRNA was diluted in serum-free medium to give a final volume of 100 µl and incubated with 1 µl RNAiFect® for 15 min at room temperature. The transfection mixture was added to the respective wells, each containing 300 µl medium (10% fetal calf serum content), to give a final concentration of 2.5 µg/ml. Transfection was performed for 24 h.

For viability analysis, cells were seeded into 96-well plates, grown to 50-80% confluence and transfected with 0.25 µg siRNA or non-silencing siRNA and 0.25 µl RNAiFect® to give a final concentration of 2.5 µg/ml.

For Western blots H4 cells were seeded in 6-well plates, grown to 50-80% confluence, and transfected with 5 µg COX-2 siRNA or non-silencing siRNA using 5 µl RNAiFect® per well. Transfection was performed for 24 h. The final concentration of siRNA or non-silencing siRNA was 2.5 µg/ml.

After transfection, cells were incubated with test substances in the presence of transfection complexes.

Statistics.

Comparisons between groups were performed with Student´s two-tailed t-test. All statistical analyses were undertaken using GraphPad Prism 3.00 (GraphPad Software, San Diego, CA, USA).

RESULTS

Time-course of R(+)-MA-induced COX-2 mRNA expression and PGE_2 synthesis.

We have recently shown that incubation of H4 human neuroglioma cells with R(+)-MA (10 µM) for up to 24 h led to a sustained increase of COX-2 mRNA that peaked at 8 h (Ramer et al., 2003). Significant elevations of PGE_2 levels were registered after incubation periods of 12 and 24 hours, respectively (Ramer et al., 2003). Analysis of a broader time frame performed for the purpose of this study revealed that significant inductions of COX-2 mRNA expression and PGE_2 synthesis were still evident following longer incubation periods. Accordingly, COX-2 mRNA levels in cells treated with R(+)-MA for 48 and 72 h were 231% ± 25% (n = 3; $P < 0.05$, vs. vehicle; Student´s *t*-test) and 226% ± 6% (n = 3; $P < 0.001$, vs. vehicle; Student´s *t*-test), respectively, relative to COX-2 mRNA levels in vehicle-treated cells (100%). PGE_2 levels determined in supernatants of cells incubated with R(+)-MA for 48 and 72 h were 433% ± 70% (n = 4; $P < 0.01$, vs. vehicle; Student´s *t*-test) and 426% ± 78% (n = 4; $P < 0.01$, vs. vehicle; Student´s *t*-test), respectively, relative to PGE_2 concentrations in supernatants of vehicle-treated cells (100%).

Time- and concentration-dependent effect of R(+)-MA on the viability and apoptosis of H4 cells.

Analysis of cell viability by the WST-1 colorimetric assay revealed a time- and concentration-dependent cytotoxic effect of R(+)-MA on H4 cells (Fig. 1A, C). The lowest survival rate was observed as an approximate 62% decrease in cell viability after a 72-h treatment with 10 µM R(+)-MA (Fig. 1A). A 48-h treatment with the same R(+)-MA concentration caused a 26% reduction in cell viability (Fig. 1A).

Molecular Pharmacology Fast Forward. Published on September 10, 2004 as DOI: 10.1124/mol.104.002618
This article has not been copyedited and formatted. The final version may differ from this version.

To determine whether R(+)-MA-induced cell death was a result of apoptosis, cytoplasmic histone-associated DNA fragments were determined as a characteristic biochemical feature of apoptotic cell death. As shown in Fig. 1A, R(+)-MA led to significantly increased cytoplasmic levels of DNA fragments following 48- and 72-h incubation periods, respectively. R(+)-MA displayed a concentration-dependent effect on DNA fragmentation (Fig. 1B).

Analysis of DNA fragments in supernatants as an index of necrosis revealed only a marginally significant (P = 0.0521, Student´s t-test) increase in cultures treated with R(+)-MA for 72 h (Fig. 1A).

Influence of celecoxib and other COX-2 inhibitors on R(+)-MA-induced apoptotic cell death.

To test a possible relationship between induction of COX-2 expression and apoptotic cell death elicited by R(+)-MA, the effect of the selective COX-2 inhibitor, celecoxib, on R(+)-MA-induced apoptotis and cell death was examined. For this purpose, H4 cells were treated with R(+)-MA in the presence or absence of celecoxib. Following a 24-h incubation of H4 cells with vehicle and R(+)-MA, respectively, average PGE_2 concentrations measured in cell culture supernatants were 0.038 µmol/L medium and 0.24 µmol/L medium, respectively (Fig. 2A). Coincubation of R(+)-MA with celecoxib (0.01-1 µM) concentration-dependently diminished R(+)-MA-induced PGE_2 formation (Fig. 2A) and afforded a concentration-dependent protection against R(+)-MA-induced DNA fragmentation (Fig. 2B) and glioma cell death (Fig. 2C). Incubation of cells with celecoxib without concomitant treatment with R(+)-MA had no significant effect on both accumulation of cytoplasmic DNA fragments and cellular viability (Fig. 2B, C).

Molecular Pharmacology Fast Forward. Published on September 10, 2004 as DOI: 10.1124/mol.104.002618
This article has not been copyedited and formatted. The final version may differ from this version.

H4 cells were also protected from R(+)-MA-induced apoptosis and cell death by the selective COX-2 inhibitor NS-398 and the preferential COX-2 inhibitor diclofenac (Fig. 3). In contrast, the specific COX-1 inhibitor SC-560 failed to prevent apoptosis and loss of cell viability caused by R(+)-MA treatment (data not shown).

Influence of celecoxib on R(+)-MA-induced changes of nuclear morphology.

We further studied the morphology of nuclei in H4 cells by staining treated cells with the cell-permeable DNA dye bisbenzimide. Bisbenzimide binds to chromatin, allowing fluorescent visualization of normal and condensed chromatin. Cells undergoing apoptosis exhibit smaller and brighter nuclei because of chromatin condensation. Treatment of cells with 10 µM R(+)-MA for 48 h (Fig. 4B) increased the number of cells exhibiting nuclear condensation compared with cells treated with vehicle alone (Fig. 4A). H4 cells that were incubated with R(+)-MA in the presence of celecoxib at 1 µM (Fig. 4C) showed similar nuclear morphology as cells treated with vehicle. In contrast, nuclear chromatin condensation induced by treatment of cells with R(+)-MA was not prevented by concomitant incubation with SC-560 (Fig. 4D).

Influence of COX-2 siRNA on R(+)-MA-induced apoptotic cell death.

The involvement of COX-2 in R(+)-MA-induced cell death was confirmed by experiments showing that transfection of cells with COX-2 siRNA significantly inhibited both DNA fragmentation and cell death by the endocannabinoid derivative (Fig. 5C). At the concentration tested COX-2 siRNA was shown to interfere with R(+)-MA-induced COX-2 mRNA (Fig. 5C) and protein expression (Fig. 5A). In contrast, incubation of cells with R(+)-MA and COX-2 siRNA both alone and in combination was without any effect on COX-1 protein expression (Fig. 5A). Control experiments revealed no significant effect of non-silencing siRNA on all parameters investigated (Fig. 5B, D).

Role of ceramide in R(+)-MA-induced apoptotic cell death.

Ceramide has recently been shown to be involved in COX-2 expression by R(+)-MA in H4 neuroglioma cells (Ramer et al., 2003). Likewise, C_2-ceramide was shown to induce COX-2 expression, whereas dihydro-C_2-ceramide was virtually inactive in this respect (Ramer et al., 2003). To investigate the impact of this upstream target conferring COX-2 expression, further experiments were performed using the ceramide synthase inhibitor fumonisin B_1 and the cell-permeable short-chain ceramide analogue, C_2-ceramide. As shown in Fig. 6A, fumonisin B_1 led to a significant inhibition of R(+)-MA-induced apoptosis and cell death. Moreover, the proapoptotic and cytotoxic effect of R(+)-MA was mimicked by C_2-ceramide (Fig. 6B). In contrast, dihydro-C_2-ceramide being used as a negative control did not significantly alter cytoplasmic levels of DNA fragments and viability of H4 cells (Fig. 6B). A possible necrotic effect of C_2-ceramide over the investigated time period was excluded by analysis of DNA fragments in supernatants (data not shown).

Role of cannabinoid and vanilloid receptors in R(+)-MA-induced apoptotic cell death.

To examine whether the inhibitory effect of R(+)-MA on H4 cell viability might be the result of a cannabinoid- or vanilloid receptor-mediated pathway, experiments using the selective CB_1 receptor antagonist, AM-251, the selective CB_2 receptor antagonist, AM-630 and the VR_1 receptor antagonist, capsazepine, were performed. However, all three compounds (tested at 1 µM) left the cytotoxic and proapoptotic effect of R(+)-MA virtually unaltered (Table 1). The same applies to the combined treatment of cells with the cannabinoid receptor antagonists (Table 1).

Molecular Pharmacology Fast Forward. Published on September 10, 2004 as DOI: 10.1124/mol.104.002618
This article has not been copyedited and formatted. The final version may differ from this version.

Effect of prostaglandin E_2 on the viability and apoptosis of H4 cells.

To determine whether the major COX-2 product, PGE_2, induces apoptotic cell death, H4 cells were incubated with increasing concentrations of PGE_2 and monitored for cytoplasmic DNA fragments and cell viability. As shown in Fig. 7, PGE_2 caused a concentration-dependent accumulation of DNA fragments (Fig. 7A) accompanied by a concentration-dependent loss of cellular viability (Fig. 7B). The administered concentrations of PGE_2 were within the range of PGE_2 concentrations observed in R(+)-MA-treated cells (Fig. 2A).

Effect of other cannabinoids on cellular viability and apoptosis of H4 cells.

To determine whether the contribution of COX-2 expression to apoptosis of H4 human neuroglioma cells was unique for R(+)-MA or shared by other cannabinoids, additional experiments were performed with the structurally related anandamide and the phytocannabinoid Δ^9-THC. In recent studies, both cannabinoids were shown to induce COX-2 expression and subsequent PGE_2 synthesis in H4 human neuroglioma cells (Ramer et al., 2001; Ramer et al., 2003). According to our results, selective COX-2 inhibition by celecoxib significantly interfered with DNA fragmentation and cell death elicited by anandamide (Fig. 8). On the other hand, celecoxib caused only a partial and not significant inhibition of Δ^9-THC-induced apoptosis and cell death (Table 2). In additional experiments, both Δ^9-THC-induced DNA fragmentation and cell death were neither prevented by selective antagonists of CB_1- and CB_2 receptors nor by a combination of both antagonists (Table 2).

Molecular Pharmacology Fast Forward. Published on September 10, 2004 as DOI: 10.1124/mol.104.002618
This article has not been copyedited and formatted. The final version may differ from this version.

DISCUSSION

Recent investigations from our group have shown that R(+)-MA induces COX-2 expression in human neuroglioma cells (Ramer et al., 2001; Ramer et al., 2003). However, the functional consequence remained to be established. The present study addressed this issue and assessed the influence of COX-2-dependent prostanoids induced by R(+)-MA on the viability and apoptosis of H4 cells.

Results from the present study are the first to show that newly expressed COX-2 contributes to the apoptotic effect of a cannabinoid on glioma cells. There are several lines of evidence supporting this notion: First, significant elevations of COX-2 mRNA and PGE_2 were observed at the time of maximum apoptosis and cell death. Second, inhibition of R(+)-MA-induced PGE_2 formation with the selective COX-2 inhibitor celecoxib was associated with a concentration-dependent increase of the survival rate of R(+)-MA-treated cells, whereas the selective COX-1 inhibitor SC-560 was inactive in this respect. Analysis of histone-complexed DNA fragments and nuclear chromatin condensation revealed a high proportion of cells undergoing apoptosis after R(+)-MA treatment, suggesting that R(+)-MA toxicity in neuroglioma cells is predominantly due to apoptotic cell death. Inhibition of COX-2 activity by celecoxib was shown to prevent cells from R(+)-MA-induced formation of cytoplasmic DNA fragments and nuclear chromatin condensation, whereas, again, the COX-1 selective inhibitor SC-560 had no such effect. Furthermore, H4 cells were also protected from R(+)-MA-induced apoptotic death by other selective (NS-398) or preferential (diclofenac) COX-2 inhibitors. Third, transfection of cells with COX-2 siRNA mimicked the inhibitory effect of celecoxib on R(+)-MA-induced apoptotic cell death. The specificity of COX-2 siRNA action was confirmed in Western blots showing downregulation of COX-2 expression without any effect on COX-1 protein levels. Fourth, apoptotic cell death was also elicited by PGE_2, the

Molecular Pharmacology Fast Forward. Published on September 10, 2004 as DOI: 10.1124/mol.104.002618
This article has not been copyedited and formatted. The final version may differ from this version.

major prostanoid of the COX-2 pathway (Hinz et al., 2000), at concentrations that were well within the PGE_2 levels determined in supernatants of R(+)-MA-treated cells. Fifth, celecoxib also significantly interfered with the proapoptotic action of the endocannabinoid anandamide, which shares the capacity of R(+)-MA to induce COX-2 expression in H4 cells (Ramer et al., 2003).

Recently, the lipid messenger ceramide has been implicated in R(+)-MA-induced COX-2 expression (Ramer et al., 2003). In the latter study, the ceramide synthase inhibitor, fumonisin B_1, was shown to suppress COX-2 expression by R(+)-MA. In the present work, further support for a proapoptotic function of COX-2 was provided by experiments demonstrating that fumonisin B_1 also caused a significant inhibition of R(+)-MA-induced apoptotic cell death. Moreover, increased cell death was observed in the presence of the cell-permeable short-chain ceramide analogue, C_2-ceramide, which also induces COX-2 in H4 cells (Ramer et al., 2003). In contrast, dihydro-C_2-ceramide being used as a negative control left cellular viability virtually unaltered. Overall, these results are in line with studies showing that the apoptotic effect of cannabinoids in glial cells relies on increased ceramide generation by the enzyme ceramide synthase (Galve-Roperh et al., 2000; Gomez del Pulgar et al., 2002).

Additional experiments addressed the issue of a functional role for cannabinoid and vanilloid receptors in R(+)-MA-induced neuroglioma cell death. Recently, the phytocannabinoid Δ^9-THC has been demonstrated to reduce the viability of C6 rat glioma cells by a mechanism involving both CB_1 and CB_2 receptors (Galve-Roperh et al., 2000). On the other hand, the endocannabinoids anandamide and 2-arachidonoylglycerol have been shown to mediate their antiproliferative action in these cells by a mechanism involving combined activation of vanilloid and cannabinoid receptors (Jacobsson et al., 2001). However, in the present study no evidence for a functional linkage between the proapoptotic action of R(+)-MA and activation of either cannabinoid or vanilloid receptors was obtained. These data support recent

observations showing that induction of COX-2 expression by R(+)-MA in H4 cells involves alternative receptor-independent signalling pathways (Ramer et al., 2001; Ramer et al., 2003). Further experiments revealed that apoptotic cell death elicited by Δ^9-THC was likewise linked to a mechanism independent of cannabinoid receptor activation. However, in contrast to R(+)-MA and anandamide, Δ^9-THC-induced apoptotic cell death was only partially and not significantly inhibited by celecoxib, suggesting that COX-2-dependent pathways play a minor role in this response. These data support results of other groups that argue for rather different molecular mechanisms underlying apoptosis and cell growth inhibition by plant-derived, synthetic and endogenous cannabinoids (Jacobsson et al., 2001). However, the exact mechanism by which Δ^9-THC causes apoptotic death of H4 cells has to be addressed in future studies.

The results of our study raise one important question. As a matter of fact, our data are in contrast to compelling evidence implying a contribution of COX-2-dependent PGs to carcinogenesis (for review see Gupta and DuBois, 2001; Chan et al., 2002; Subbaramaiah and Dannenberg, 2003). Accordingly, overexpression of COX-2 in epithelial cells has been shown to result in resistance to apoptosis (Tsujii and DuBois, 1995). Moreover, COX-2-derived PGs may modulate the production of angiogenic factors, thereby inducing newly formed blood vessels that sustain tumour growth (Tsujii and DuBois, 1995). In rodent models of familial adenomatous polyposis, genetic deletion of COX-2 suppressed intestinal polyp formation (Oshima et al., 1996). Population-based studies have established that chronic intake of non-steroidal anti-inflammatory drugs (NSAIDs) provides a 40- to 50% reduction in relative risk of death by colon cancer (for review see Gupta and DuBois, 2001). Meanwhile, selective inhibition of COX-2 has been implicated as an effective strategy for treatment of patients with cancer or familial adenomatous polyposis (Steinbach et al., 2000). Likewise, treatment of various cancer cell lines with specific COX-2 inhibitors has been associated with inhibition of

cell growth and induction of apoptosis. For example, growth inhibition of human cancer cells by a selective COX-2 inhibitor has been linked to inhibition of COX-2 activity and decreased synthesis of PGE_2, the latter conferring increased clonogenicity and decreased apoptosis of these cells (Sheng et al., 1998). However, this issue deserves further discussion in that most in vitro studies focused on the single effects of NSAIDs on the proliferation of cancer cells using suprapharmacological concentrations of these drugs (Zhang et al., 1999; Grosch et al., 2001; Hwang et al., 2002; Denkert et al., 2003). In particular, high concentrations of celecoxib and other NSAIDs were shown to retain their proapoptotic and antiproliferative properties in cells that do not express COX-2 (Zhang et al., 1999; Grosch et al., 2001; Hwang et al., 2002; Denkert et al., 2003), suggesting that the anti-cancer activity of these compounds might also reflect COX-independent effects.

In our hands celecoxib inhibited R(+)-MA-induced apoptosic cell death at concentrations that were well within the pharmacological range of concentrations obtained in plasma of patients receiving celecoxib. Accordingly, single dose administration of celecoxib at 100, 400 or 800 mg yielded maximal plasma concentrations of 1.44, 2.54 and 7.67 µM, respectively (McAdam et al., 1999). At the concentrations tested in the present work, celecoxib itself did not induce apoptosis or cell death. On the other hand, the same concentrations of celecoxib were found to concentration-dependently interfere with the proapoptotic and cytotoxic action of R(+)-MA. These data are consistent with other reports. Accordingly, the selective COX-2 inhibitor NS-398 has recently been shown to inhibit the proapoptotic and antiproliferative effect of paclitaxel, a frequently used chemotherapeutic agent, on epithelial ovarian cancer cells (Munkarah et al., 2003). Noteworthy, taxanes have been demonstrated to upregulate COX-2 expression in different cells (Moos et al., 1999; Subbaramaiah et al., 2000). In another study, the apoptotic death of human mammary epithelial cells elicited by the chemotherapeutic edelfosine was attenuated by celecoxib (Na and Surh, 2002). More recently,

the growth of colon carcinoma Caco-2 cells stimulated by polyunsaturated fatty acids was found to be enhanced by indomethacin, partially through inhibition of peroxidation products generated by the COX pathway (Dommels et al., 2003). Furthermore, the proapoptotic action of the endocannabinoid-like compound stearoylethanolamide on C6 cells was shown to be associated with activation of prostaglandin formation (Maccarrone et al., 2002).

Collectively, these data as well as the results of the present study raise the intriguing question, whether the use of COX inhibitors prior to or concurrently with COX-2-inducing chemotoxic agents may attenuate the therapeutic efficacy of these compounds. This issue merits further investigation given that COX inhibitors are often co-administered during cancer treatment, but also unknowingly used by cancer patients for pain reduction.

In conclusion, the present study suggests that R(+)-MA and anandamide cause apoptotic death of H4 neuroglioma cells by a mechanism involving de novo expression of COX-2. As cannabinoids and inhibitors of endocannabinoid inactivation have been implicated as anti-tumorigenic substances (Guzman et al., 2001; Bifulco et al., 2004), our results defining COX-2 as a novel target in the regulation of cell fate by R(+)-MA and anandamide shed light on an important step within this process. Moreover, our data show that suppression of COX-2 activity by pharmacological concentrations of the selective COX-2 inhibitor celecoxib is accompanied by an inhibition of the proapoptotic action of R(+)-MA and anandamide on H4 neuroglioma cells, suggesting that co-treatment with COX-2 inhibitors could diminish the glioma-regressing effect of these cannabinoids.

REFERENCES

Bagetta G, Corasaniti MT, Paoletti AM, Berliocchi L, Nistico R, Giammarioli AM, Malorni W, and Finazzi-Agro A (1998) HIV-1 gp120-induced apoptosis in the rat neocortex involves enhanced expression of cyclo-oxygenase type 2 (COX-2). *Biochem Biophys Res Commun* **244:**819-824.

Bifulco M, Laezza C, Valenti M, Ligresti A, Portella G, and Di Marzo V (2004) A new strategy to block tumor growth by inhibiting endocannabinoid inactivation. *FASEB J* Aug 2 [Epub ahead of print]

Burstein SH, Hull K, Hunter SA, and Shilstone J (1989) Immunization against prostaglandins reduces Δ^1-tetrahydrocannabinol-induced catalepsy in mice. *Mol Pharmacol* **35:**6-9.

Chan GC, Hinds TR, Impey S, and Storm DR (1998) Hippocampal neurotoxicity of Δ^9-tetrahydrocannabinol. *J Neurosci* **18:**5322-5332.

Chan TA (2002) Nonsteroidal anti-inflammatory drugs, apoptosis, and colon-cancer chemoprevention. *Lancet Oncol* **3:**166-174.

Denkert C, Fürstenberg A, Daniel PT, Koch I, Köbel M, Weichert W, Siegert A, and Hauptmann S (2003) Induction of G0/G1 cell cycle arrest in ovarian carcinoma cells by the anti-inflammatory drug NS-398, but not by COX-2-specific RNA interference. *Oncogene* **22:**8653-8661.

Dommels YE, Haring MM, Keestra NG, Alink GM, van Bladeren PJ, and van Ommen B (2003) The role of cyclooxygenase in n-6 and n-3 polyunsaturated fatty acid mediated effects on cell proliferation, PGE_2 synthesis and cytotoxicity in human colorectal carcinoma cell lines. *Carcinogenesis* **24:**385-392.

Elbashir SM, Harborth J, Weber K, and Tuschl T (2002) Analysis of gene function in somatic mammalian cells using small interfering RNAs. *Methods* **26:**199-213.

Ellis EF, Moore SF, and Willoughby KA (1995) Anandamide and Δ^9-THC dilation of cerebral arterioles is blocked by indomethacin. *Am J Physiol* **269:**H1859-H1864.

Galve-Roperh I, Sanchez C, Cortes ML, del Pulgar TG, Izquierdo M and Guzman M (2000) Anti-tumoral action of cannabinoids**:** involvement of sustained ceramide accumulation and extracellular signal-regulated kinase activation. *Nat Med* **6:**313-319.

Gomez del Pulgar T, Velasco G, Sanchez C, Haro A, and Guzman M (2002) De novo-synthesized ceramide is involved in cannabinoid-induced apoptosis. *Biochem J* **363:**183-188.

Green K, Kearse EC, and McIntyre OL (2001) Interaction between Δ^9-tetrahydrocannabinol and indomethacin. *Ophthalmic Res* **33:**217-220.

Grosch S, Tegeder I, Niederberger E, Brautigam L, and Geisslinger G (2001) COX-2 independent induction of cell cycle arrest and apoptosis in colon cancer cells by the selective COX-2 inhibitor celecoxib. *FASEB J* **15:**2742-2744.

Gupta RA and DuBois RN (2001) Colorectal cancer prevention and treatment by inhibition of cyclooxygenase-2. *Nat Rev Cancer* **1:**11-21.

Guzman M, Galve-Roperh I, and Sanchez C (2001) Ceramide**:** a new second messenger of cannabinoid action. *Trends Pharmacol Sci* **22:**19-22.

Hinz B and Brune K (2002) Cyclooxygenase-2 – Ten years later. *J Pharmacol Exp Ther* **300:**367-375.

Hinz B, Brune K, and Pahl A (2000) Cyclooxygenase-2 expression in lipopolysaccharide-stimulated human monocytes is modulated by cyclic AMP, prostaglandin E_2, and nonsteroidal anti-inflammatory drugs. *Biochem Biophys Res Commun* **278:**790-796.

Hwang DH, Fung V, and Dannenberg AJ (2002) National Cancer Institute workshop on chemopreventive properties of nonsteroidal anti-inflammatory drugs**:** role of COX-dependent and -independent mechanisms. *Neoplasia* **4:**91-97.

Jacobsson SO, Wallin T, and Fowler CJ (2001) Inhibition of rat C6 glioma cell proliferation by endogenous and synthetic cannabinoids. Relative involvement of cannabinoid and vanilloid receptors. *J Pharmacol Exp Ther* **299:**951-959.

Jayanthi S, Lewis BD, and Cadet JL (2001) Fas-induced apoptosis of glioma cells is associated with down-regulation of the hSCO1 protein, a subunit of complex IV. *Brain Res Mol Brain Res* **91:**131-136.

Kim TA, Ota S, Jiang S, Pasztor LM, White RA, and Avraham S (2000) Genomic organization, chromosomal localization and regulation of expression of the neuronal nuclear matrix protein NRP/B in human brain tumors. *Gene* **255:**105-116.

Krex D, Mohr B, Hauses M, Ehninger G, Schackert HK, and Schackert G (2001) Identification of uncommon chromosomal aberrations in the neuroglioma cell line H4 by spectral karyotyping. *J Neurooncol* **52:**119-128.

Maccarrone M, Pauselli R, Di Rienzo M, and Finazzi-Agro A (2002) Binding, degradation and apoptotic activity of stearoylethanolamide in rat C6 glioma cells. *Biochem J* **366:**137-144.

McAdam BF, Catella-Lawson F, Mardini IA, Kapoor S, Lawson JA, and FitzGerald GA (1999) Systemic biosynthesis of prostacyclin by cyclooxygenase (COX)-2**:** the human pharmacology of a selective inhibitor of COX-2. *Proc Natl Acad Sc. USA* **96:**272-277.

Moore RM, Lundgren DW, and Moore JJ (1999) Cyclooxygenase inhibitors decrease apoptosis initiated by actinomycin D, cycloheximide, and staurosporine in amnion-derived WISH cells. *J Soc Gynecol Invest* **6:**245-251.

Moos PJ, Muskardin DT, and Fitzpatrick FA (1999) Effect of taxol and taxotere on gene expression in macrophages**:** induction of the prostaglandin H synthase-2 isoenzyme. *J Immunol* **162:**467-473.

Munkarah AR, Genhai Z, Morris R, Baker VV, Deppe G, Diamond MP, and Saed GM (2003) Inhibition of paclitaxel-induced apoptosis by the specific COX-2 inhibitor, NS398, in epithelial ovarian cancer cells. *Gynecol Oncol* **88:**429-433.

Munson AE, Harris LS, Friedman MA, Dewey WL, and Carchman RA (1975) Antineoplastic activity of cannabinoids. *J Natl Cancer Inst* **55:**597-602.

Na HK and Surh YJ (2002) Induction of cyclooxygenase-2 in Ras-transformed human mammary epithelial cells undergoing apoptosis. *Ann N Y Acad Sci* **973:**153-160.

Oshima M, Dinchuk JE, Kargman SL, Oshima H, Hancock B, Kwong E, Trzaskos JM, Evans JF, and Taketo MM (1996) Suppression of intestinal polyposis in *Apc*$^{\Delta 716}$ knockout mice by inhibition of cyclooxygenase 2 (COX-2). *Cell* **87:**803-809.

Perez-Reyes M, Burstein SH, White WR., McDonald SA, and Hicks RE (1991) Antagonism of marihuana effects by indomethacin in humans. *Life Sci* **48:**507-515.

Ramer R, Brune K, Pahl A, and Hinz B (2001) R(+)-methanandamide induces cyclooxygenase-2 expression in human neuroglioma cells via a non-cannabinoid receptor-mediated mechanism. *Biochem Biophys Res Commun* **286:**1144-1152.

Ramer R, Weinzierl U, Schwind B, Brune K, and Hinz B (2003) Ceramide is involved in R(+)-methanandamide-induced cyclooxygenase-2 expression in human neuroglioma cells. *Mol Pharmacol* **64:**1189-1198.

Sheng H, Shao J, Morrow JD, Beauchamp RD, and DuBois RN (1998) Modulation of apoptosis and Bcl-2 expression by prostaglandin E_2 in human colon cancer cells. *Cancer Res* **58:**362-366.

Steinbach G, Lynch PM, Phillips RK, Wallace MH, Hawk E, Gordon GB, Wakabayashi N, Saunders B, Shen Y, Fujimura T, Su LK, and Levin B (2000) The effect of celecoxib, a cyclooxygenase-2 inhibitor, in familial adenomatous polyposis. *N Engl J Med* **342:**1946-1952.

Subbaramaiah K and Dannenberg AJ (2003) Cyclooxygenase 2: a molecular target for cancer prevention and treatment. *Trends Pharmacol Sci* **24:**96-102.

Subbaramaiah K, Hart JC, Norton L, and Dannenberg AJ (2000) Microtubule-interfering agents stimulate the transcription of cyclooxygenase-2. Evidence for involvement of ERK1/2 AND p38 mitogen-activated protein kinase pathways. *J Biol Chem* **275:**14838-14845.

Tsujii M and DuBois RN (1995) Alterations in cellular adhesion and apoptosis in epithelial cells overexpressing prostaglandin endoperoxide synthase-2. *Cell* **83:**493-501.

Yamaguchi T, Shoyama Y, Watanabe S, and Yamamoto T (2001) Behavioral suppression induced by cannabinoids is due to activation of the arachidonic acid cascade in rats. *Brain Res* **889:**149-154.

Zhang X, Morham SG, Langenbach R, and Young DA (1999) Malignant transformation and antineoplastic actions of nonsteroidal antiinflammatory drugs (NSAIDs) on cyclooxygenase-null embryo fibroblasts. *J Exp Med* **190:**451-459.

Footnotes: # This study was supported by the Deutsche Forschungsgemeinschaft (HI 813/1-1 and SFB 539, BI.6).

Send reprint requests to: Dr. Burkhard Hinz, Department of Experimental and Clinical Pharmacology and Toxicology, Friedrich Alexander University Erlangen-Nürnberg, Fahrstrasse 17, D-91054 Erlangen, Germany

FIGURE LEGENDS

Figure 1

Time- (A) and concentration-dependent (B, C) effect of R(+)-MA on cytoplasmic DNA fragmentation and viability of H4 human neuroglioma cells. Cells were incubated with R(+)-MA or its vehicle for the indicated times (A), for 48 h (B) or for 72 h (C). For time-course experiments (A) accumulation of histone-associated DNA fragments in both the cytoplasm (apoptosis marker) or supernatant (necrosis marker) of H4 cells was determined. Percent control represents comparison with vehicle-treated cells (100%) in the absence of test substance. Values are means ± SEM of n = 3-4 experiments. **P* < 0.05, ***P* < 0.01, ****P* < 0.001 vs. corresponding vehicle control, Student´s *t*-test.

Figure 2

Effect of celecoxib (0.01-1 µM) on R(+)-MA-induced PGE_2 formation (A), on the accumulation of cytoplasmic DNA fragments (B) and on the viability of H4 cells (C) in the presence or absence of R(+)-MA. Cells were incubated with R(+)-MA (10 µM), celecoxib or its vehicles for 24 (A), 48 (B) or 72 h (C). Percent control represents comparison with vehicle-treated cells (100%) in the absence of test substance. Values are means ± SEM of n = 4 (A), n = 3 (B) or n = 8 (C) experiments. **P* < 0.05, ***P* < 0.01, ****P* < 0.001 vs. sole R(+)-MA treatment, unless otherwise indicated (Student´s *t*-test).

Figure 3

Effect of NS-398 (1 µM) and diclofenac (1 µM) on R(+)-MA-induced accumulation of cytoplasmic DNA fragments and subsequent death of H4 cells. Cells were incubated with the indicated substances, R(+)-MA (10 µM) or its vehicles for 48 h (DNA fragmentation) or 72 h

(cell viability). Data are shown as percentual inhibitions of R(+)-MA-induced DNA fragmentation or cell death. Values are means ± SEM of n = 3 (DNA fragmentation) or n = 4 (cell viability) experiments. *P < 0.05, **P < 0.01, ***P < 0.001 vs. sole R(+)-MA treatment (Student´s *t*-test).

Figure 4

Bisbenzimide fluorescence microscopy of H4 cells after a 48-h treatment with vehicle (A), R(+)-MA (B) or R(+)-MA in combination with 1 µM celecoxib (C) or 1 µM SC-560 (D). Bisbenzimide intercalates into DNA strands, allowing fluorescent visualization of chromatin. Normal nuclei are regular in shape and size, whereas apoptotic nuclei show condensation of chromatin material and appear smaller and round-shaped (arrows). H4 cells incubated with R(+)-MA (B) or R(+)-MA in the presence of the COX-1 inhibitor SC-560 (D) show increased numbers of nuclei with condensed chromatin material as compared to vehicle-treated H4 cells (A). Cells treated with R(+)-MA and the selective COX-2 inhibitor celecoxib (C) show similar nuclear morphology as cells treated with vehicle.

Figure 5

Effect of COX-2 siRNA (2.5 µg/ml) and non-silencing siRNA (non-sil. siRNA; 2.5 µg/ml) on COX-2 or COX-1 protein expression (A, B), COX-2 mRNA expression (C, D), DNA fragmentation (C, D) and viability of H4 cells (C, D) in the presence or absence of R(+)-MA. Cells were incubated with R(+)-MA or its vehicle for 8 h (COX-2 mRNA), 24 h (COX-2 or COX-1 protein), 48 h (DNA fragmentation) or 72 h (cell viability). Transfection with COX-2 siRNA or non-silencing siRNA was performed 24 h prior to addition of R(+)-MA to the cells. Percent control represents comparison with vehicle-treated cells (100%) in the absence of test substances. Values are means ± SEM of n = 3 (COX-2 mRNA, DNA fragmentation) or n = 4

(cell viability) experiments. **P* < 0.05, ***P* < 0.01, ****P* < 0.001, vs. indicated group (Student´s *t*-test). Results of the Western blots are representative of three experiments with similar results.

Figure 6

Effect of fumonisin B_1 (50 µM) on R(+)-MA-induced accumulation of cytoplasmic DNA fragments and subsequent death of H4 cells (A). Effect of C_2-ceramide (30 µM) and dihydro-C_2-ceramide (30 µM) on the accumulation of cytoplasmic DNA fragments and on viability of H4 cells (B). For analysis of DNA fragmentation cells were incubated with the indicated substances for 48 h (A) and 24 h (B), respectively. Incubation periods for determination of cellular viability were 72 h (A) and 48 h (B), respectively. Fumonisin B_1 was added 1 h prior to R(+)-MA. Percent control represents comparison with vehicle-treated cells (100%) in the absence of test substances. Values are means ± SEM of n = 3 (DNA fragmentation) or n = 4 (cell viability) experiments. ***P* < 0.01, ****P* < 0.001, vs. indicated group (Student´s *t*-test).

Figure 7

Effect of PGE_2 (0.01-1 µM) on the accumulation of cytoplasmic DNA fragments (A) and on the viability of H4 cells (B). Cells were incubated with PGE_2 or its vehicle for 48 h (A) or 72 h (B). Percent control represents comparison with vehicle-treated cells (100%) in the absence of test substance. Values are means ± SEM of n = 3 experiments. **P* < 0.05, ***P* < 0.01, ****P* < 0.001, vs. corresponding vehicle control (Student´s *t*-test).

Figure 8

Effect of celecoxib (1 µM) on anandamide (AEA)-induced accumulation of cytoplasmic DNA fragments and subsequent death of H4 cells. Cells were incubated with anandamide (10 µM)

or its vehicle in the absence or presence of celecoxib for 48 h (DNA fragmentation) or 72 h (cell viability). Percent control represents comparison with vehicle-treated cells (100%) in the absence of test substance. Values are means ± SEM of n = 3 (DNA fragmentation) or n = 4 (cell viability) experiments. $^{**}P < 0.01$, $^{***}P < 0.001$, vs. indicated group (Student´s *t*-test).

TABLES

Table 1

Effect of AM-251 (1 μM), AM-630 (1 μM) and capsazepine (1 μM) on R(+)-MA-induced accumulation of cytoplasmic DNA fragments and subsequent death of H4 cells. Cells were incubated with the indicated substances, R(+)-MA (10 μM) or its vehicles for 48 h (DNA fragmentation) or 72 h (cell viability). Receptor antagonists were added 1 h prior to R(+)-MA. Percent control represents comparison with vehicle-treated cells (100%) in the absence of test substances. Percent control represents comparison with vehicle-treated cells (100%) in the absence of test substance. Values are means ± SEM of n = 3 (DNA fragmentation) or n = 4 (cell viability) experiments.

	DNA fragmentation	Cell viability
	%	%
Vehicle	100 ± 5	100 ± 14
R(+)-MA	204 ± 14	59 ± 5
R(+)-MA + AM-251	173 ± 5	55 ± 7
R(+)-MA + AM-630	206 ± 11	59 ± 9
R(+)-MA + AM-251 + AM-630	182 ± 22	52 ± 11
R(+)-MA + Capsazepine	251 ± 13	58 ± 2

Table 2

Effect of celecoxib (1 μM), AM-251 (1 μM) and AM-630 (1 μM) on Δ^9-THC-induced accumulation of cytoplasmic DNA fragments and subsequent death of H4 cells. Cells were incubated with the indicated substances, Δ^9-THC (10 μM) or its vehicles for 48 h (DNA fragmentation) or 72 h (cell viability). Receptor antagonists were added 1 h prior to Δ^9-THC. Percent control represents comparison with vehicle-treated cells (100%) in the absence of test substances. Percent control represents comparison with vehicle-treated cells (100%) in the absence of test substance. Values are means ± SEM of n = 3 (DNA fragmentation) or n = 4 (cell viability) experiments.

	DNA fragmentation	Cell viability
	%	%
Vehicle	100 ± 4	100 ± 6
Δ^9-THC	299 ± 26	6 ± 0.5
Δ^9-THC + Celecoxib	227 ± 36	15 ± 5
Vehicle	100 ± 3	100 ± 4
Δ^9-THC	300 ± 40	16 ± 2
Δ^9-THC + AM-251	290 ± 46	14 ± 1
Δ^9-THC + AM-630	328 ± 43	11 ± 2
Δ^9-THC + AM-251 + AM-630	257 ± 21	19 ± 2

Molecular Pharmacology Fast Forward. Published on September 10, 2004 as DOI: 10.1124/mol.104.002618
This article has not been copyedited and formatted. The final version may differ from this version.

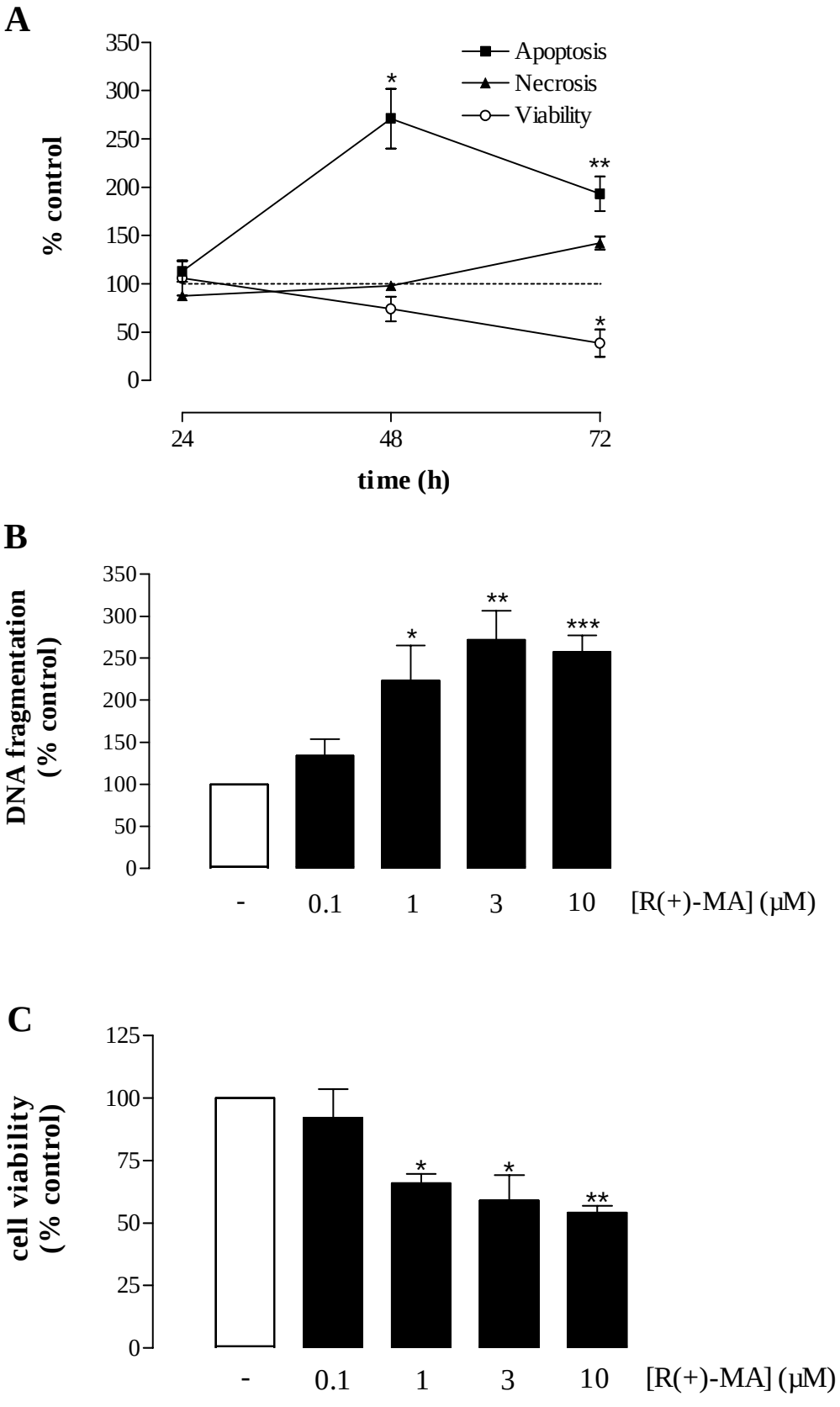

Fig. 1

Molecular Pharmacology Fast Forward. Published on September 10, 2004 as DOI: 10.1124/mol.104.002618
This article has not been copyedited and formatted. The final version may differ from this version.

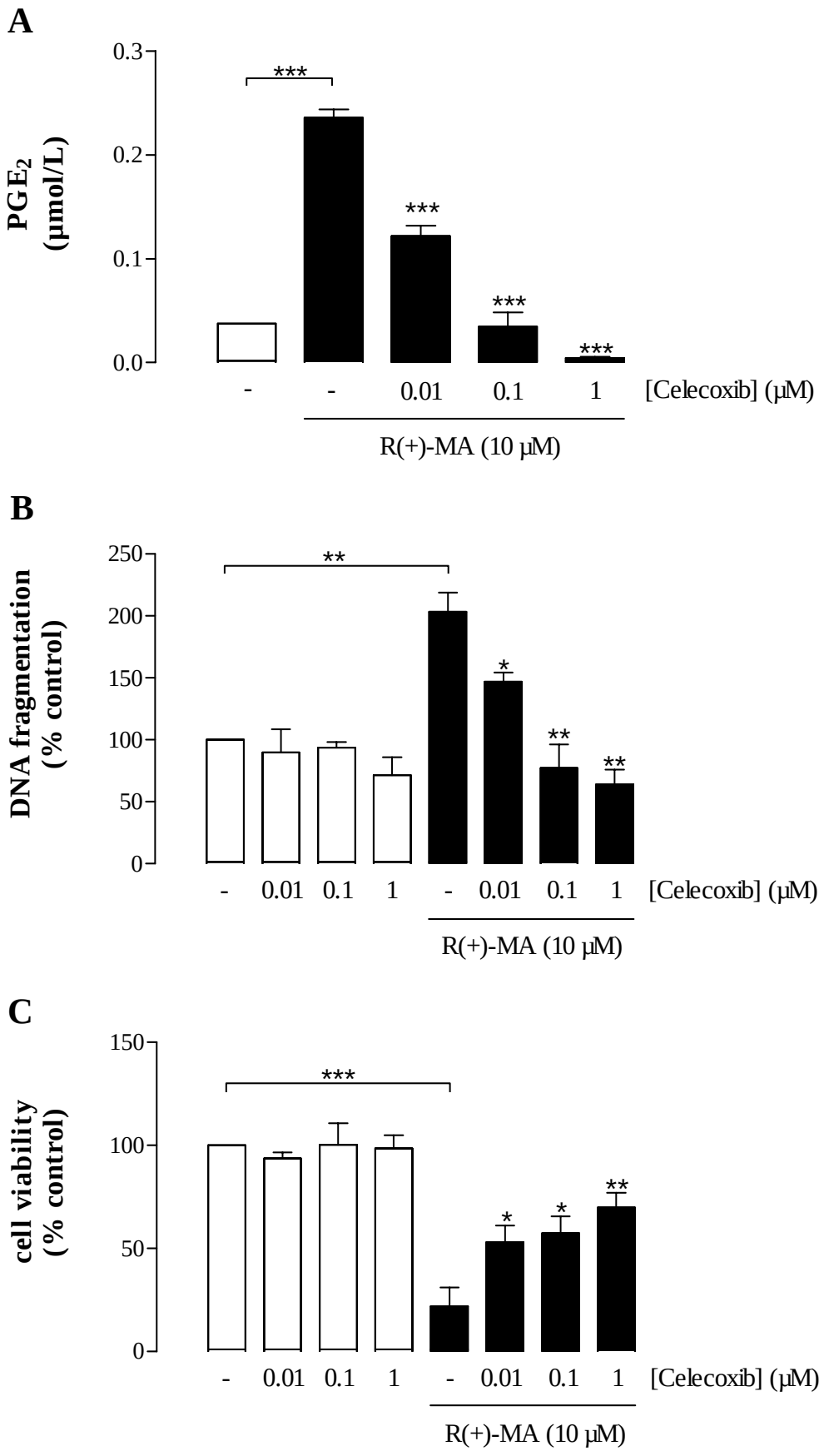

Fig. 2

Molecular Pharmacology Fast Forward. Published on September 10, 2004 as DOI: 10.1124/mol.104.002618
This article has not been copyedited and formatted. The final version may differ from this version.

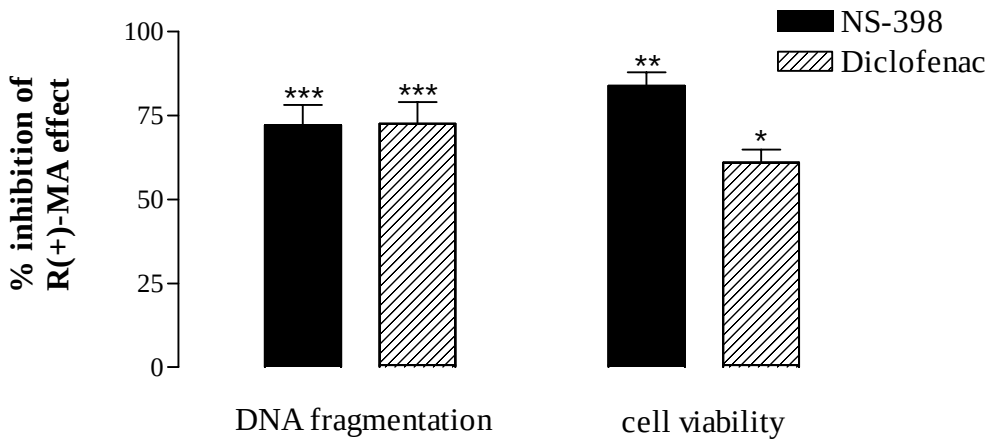

Fig. 3

Molecular Pharmacology Fast Forward. Published on September 10, 2004 as DOI: 10.1124/mol.104.002618
This article has not been copyedited and formatted. The final version may differ from this version.

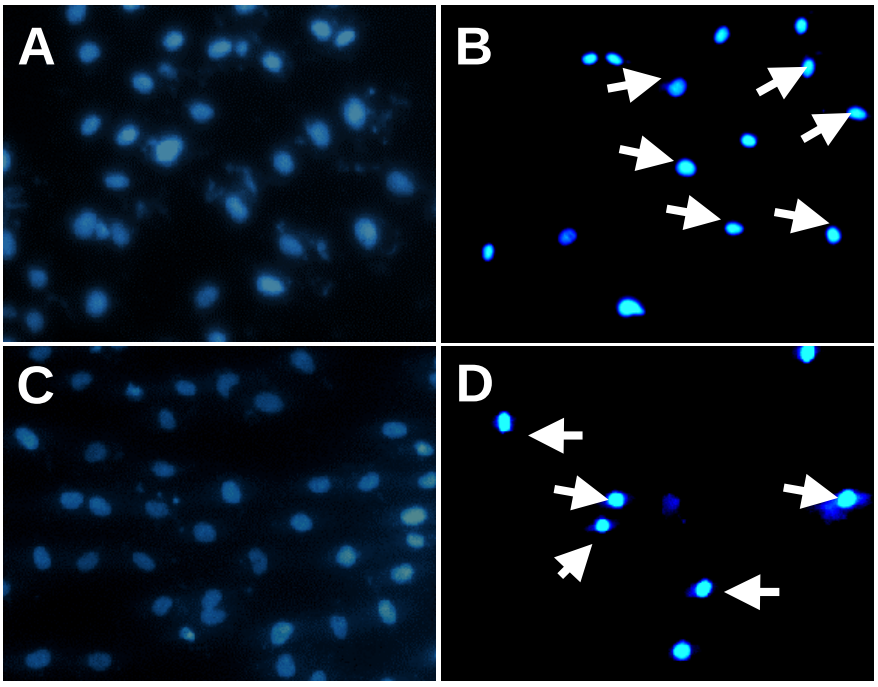

Fig. 4

Molecular Pharmacology Fast Forward. Published on September 10, 2004 as DOI: 10.1124/mol.104.002618
This article has not been copyedited and formatted. The final version may differ from this version.

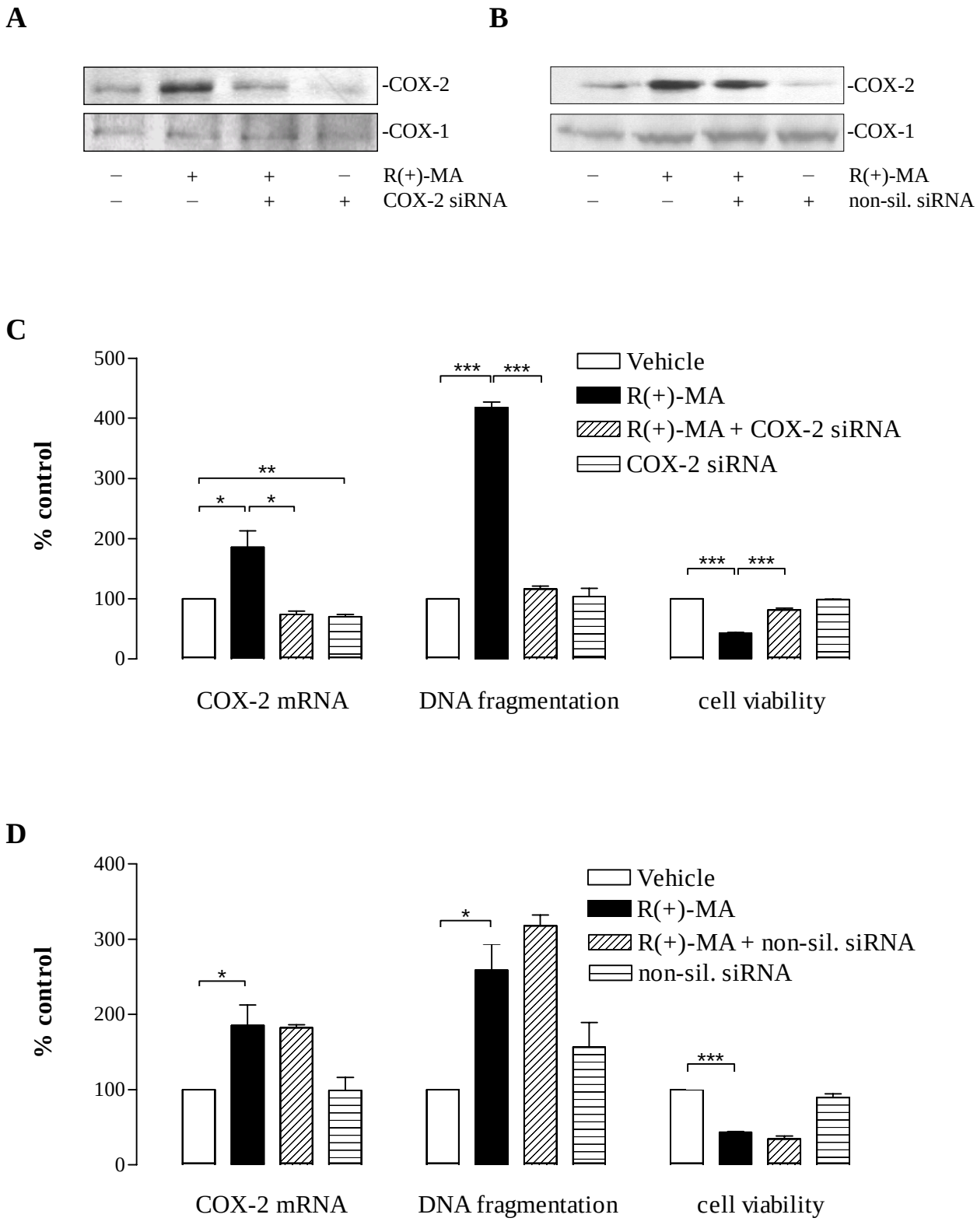

Fig. 5

Molecular Pharmacology Fast Forward. Published on September 10, 2004 as DOI: 10.1124/mol.104.002618
This article has not been copyedited and formatted. The final version may differ from this version.

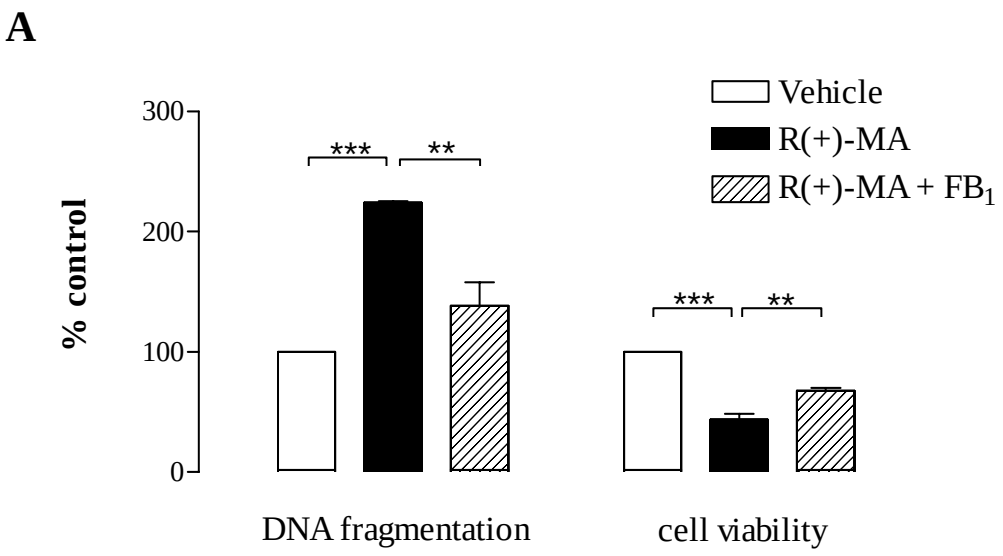

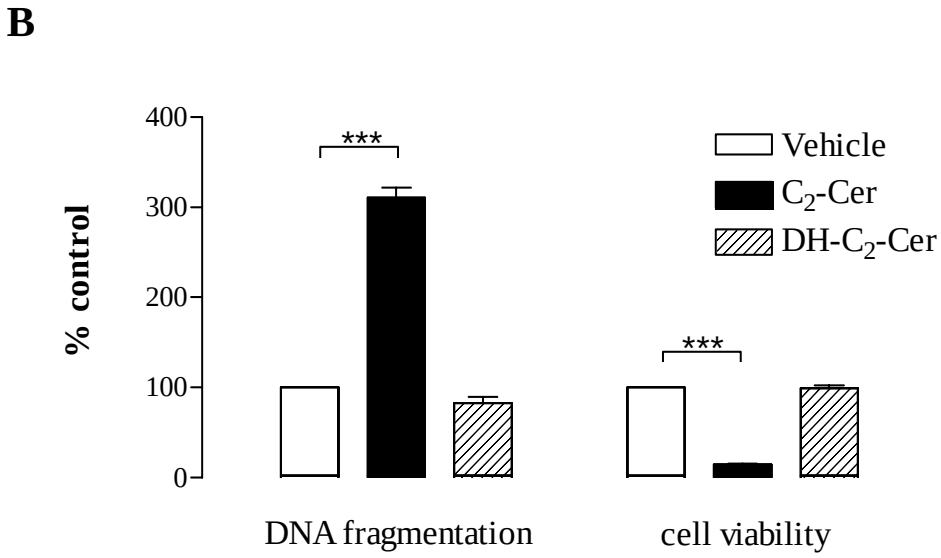

Fig. 6

Molecular Pharmacology Fast Forward. Published on September 10, 2004 as DOI: 10.1124/mol.104.002618
This article has not been copyedited and formatted. The final version may differ from this version.

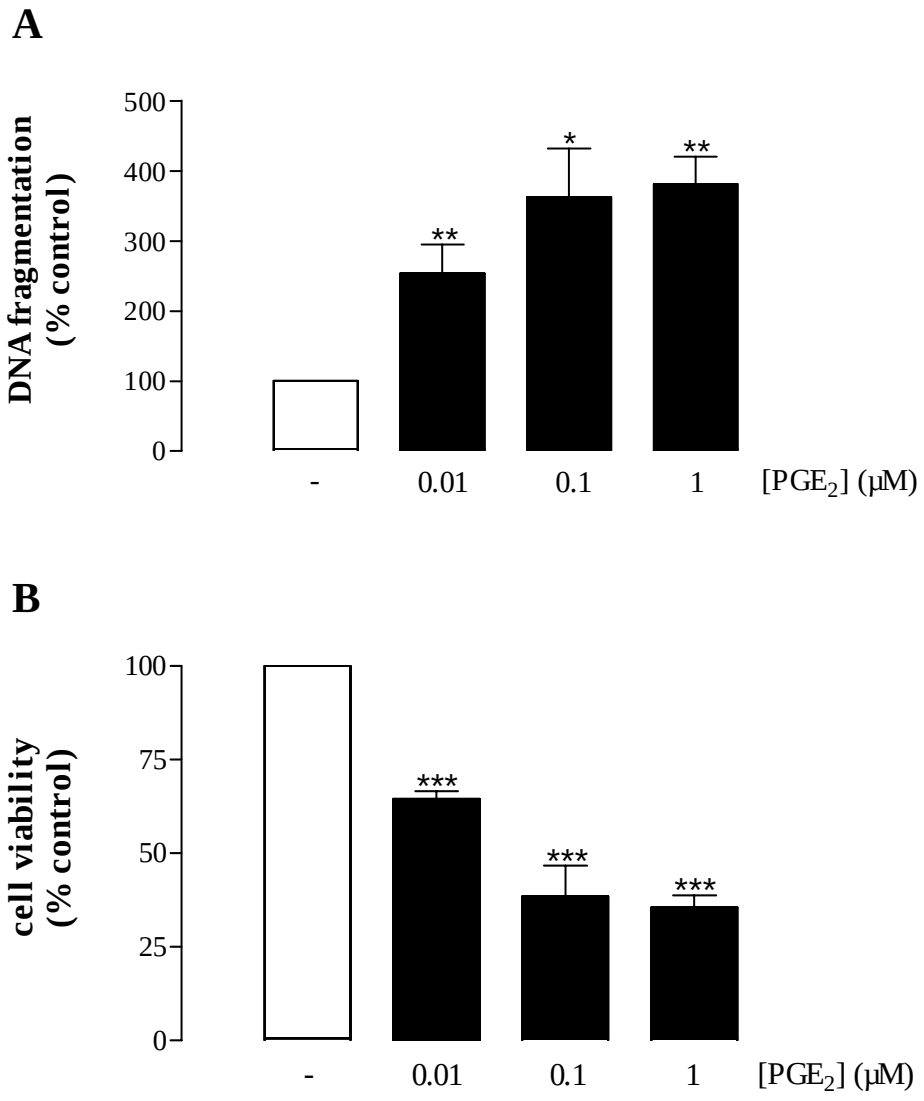

Fig. 7

Molecular Pharmacology Fast Forward. Published on September 10, 2004 as DOI: 10.1124/mol.104.002618
This article has not been copyedited and formatted. The final version may differ from this version.

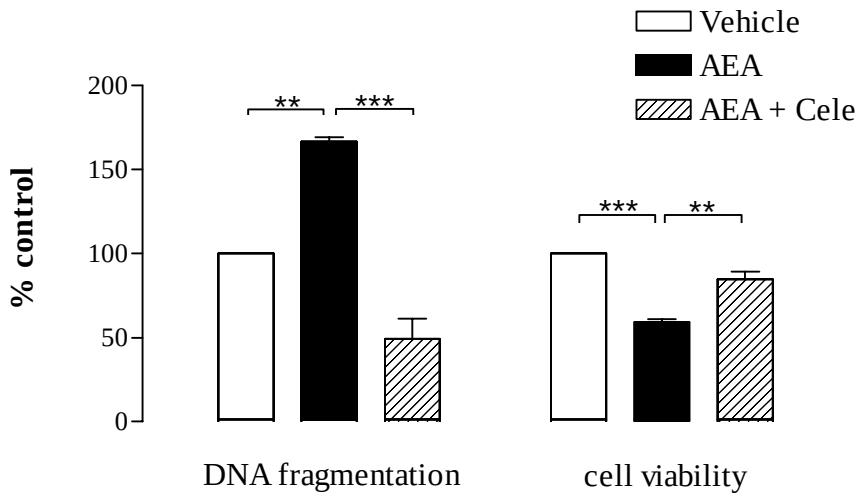

Fig. 8